Photoproduction J/ψ Detection and Physics with ECCE

X. Li[1], W. Zha[1], J. K. Adkins[36], Y. Akiba[53], A. Albataineh[69], M. Amaryan[47], I. C. Arsene[73], J. Bae[61], X. Bai[78], M. Bashkanov[87], R. Bellwied[67], F. Benmokhtar[15], J. C. Bernauer[55,56,57], F. Bock[49], W. Boeglin[17], M. Borysova[83], E. Brash[11], P. Brindza[28], W. J. Briscoe[21], M. Brooks[32], S. Bueltmann[47], M. H. S. Bukhari[27], A. Bylinkin[69], R. Capobianco[66], W.-C. Chang[3], Y. Cheon[59], K. Chen[8], K.-F. Chen[46], K.-Y. Cheng[40], M. Chiu[5], T. Chujo[76], Z. Citron[1], E. Cline[55,56], E. Cohen[44], T. Cormier[49], Y. Corrales Morales[32], C. Cotton[78], C. Crawford[70], S. Creekmore[49], C.Cuevas[28], J. Cunningham[49], G. David[5], C. T. Dean[32], M. Demarteau[49], S. Diehl[66], N. Doshita[85], R. Dupré[24], J. M. Durham[32], R. Dzhygadlo[20], R. Ehlers[49], L. El Fassi[38], A. Emmert[78], R. Ent[28], C. Fanelli[37], R. Fatemi[70], S. Fegan[87], M. Finger[9], M. Finger Jr.[9], J. Frantz[48], M. Friedman[23], I. Friscic[88], D. Gangadharan[67], S. Gardner[19], K. Gates[19], F. Geurts[52], R. Gilman[54], D. Glazier[19], E. Glimos[49], Y. Goto[53], N. Grau[4], S. V. Greene[79], A. Q. Guo[25], L. Guo[17], S. K. Ha[86], J. Haggerty[5], T. Hayward[66], X. He[18], O. Hen[37], D. W. Higinbotham[28], M. Hoballah[24], T. Horn[13], P.-h. J. Hsu[45], J. Huang[5], G. Huber[74], A. Hutson[67], K. Y. Hwang[86], C. Hyde[47], M. Inaba[64], T. Iwata[85], H.-S. Jo[31], K. Joo[66], N. Kalantarians[81], K. Kawade[60], S. J. D. Kay[74], A. Kim[66], B. Kim[61], C. Kim[51], M. Kim[53], Y. Kim[51], Y. Kim[59], E. Kistenev[5], V. Klimenko[66], S. H. Ko[58], I. Korover[37], W. Korsch[70], G. Krintiras[69], S. Kuhn[47], C.-M. Kuo[40], T. Kutz[37], J. Lajoie[26], D. Lawrence[28], S. Lebedev[26], J. S. H. Lee[58], S. W. Lee[31], Y.-J. Lee[37], W. Li[52], W. Li[55,56,84], X. Li[10], X. Li[32], Y. T. Liang[25], S. Lim[51], C.-h. Lin[3], D. X. Lin[25], K. Liu[32], M. X. Liu[32], K. Livingston[19], N. Liyanage[78], W. J. Llope[82], C. Loizides[49], E. Long[72], R.-S. Lu[46], Z. Lu[10], W. Lynch[87], D. Marchand[24], M. Marcisovsky[14], P. Markowitz[17], P. McGaughey[32], M. Mihovilovic[71], R. G. Milner[37], A. Milov[83], Y. Miyachi[85], P. Monaghan[11], R. Montgomery[19], D. Morrison[5], C. Munoz Camacho[24], M. Murray[69], K. Nagai[32], J. Nagle[65], I. Nakagawa[53], C. Nattrass[77], D. Nguyen[28], S. Niccolai[24], R. Nouicer[5], G. Nukazuka[53], M. Nycz[78], V. A. Okorokov[43], S. Orešić[74], J.D. Osborn[49], C. O'Shaughnessy[32], S. Paganis[46], Z Papandreou[74], S. Pate[42], M. Patel[26], C. Paus[37], G. Penman[19], M. G. Perdekamp[68], D. V. Perepelitsa[65], H. Periera da Costa[32], K. Peters[20], W. Phelps[11], E. Piasetzky[62], C. Pinkenburg[5], I. Prochazka[9], T. Protzman[34], M. Purschke[5], J. Putschke[82], J. R. Pybus[37], R. Rajput-Ghoshal[28], J. Rasson[49], B. Raue[17], K. Read[49], K. Røed[73], R. Reed[34], J. Reinhold[17], E. L. Renner[32], J. Richards[66], C. Riedl[68], T. Rinn[5], J. Roche[48], G. M. Roland[37], G. Ron[23], M. Rosati[26], C. Royon[69], J. Ryu[51], S. Salur[54], N. Santiesteban[37], R. Santos[66], M. Sarsour[18], J. Schambach[49], A. Schmidt[21], N. Schmidt[49], C. Schwarz[20], J. Schwiening[20], R. Seidl[53], A. Sickles[68], P. Simmerling[66], S. Sirca[71], D. Sharma[18], Z. Shi[32], T.-A. Shibata[41], C.-W. Shih[40], S. Shimizu[53], U. Shrestha[66], K. Slifer[72], K. Smith[32], R. Soltz[35], W. Sondheim[32], J. Song[10], J. Song[51], I. I. Strakovsky[21], P. Steinberg[5], J. Stevens[84], J. Strube[50], P. Sun[10], X. Sun[8], K. Suresh[74], W.-C. Tang[40], S. Tapia Araya[26], S. Tarafdar[79], L. Teodorescu[6], A. Timmins[67], L. Tomasek[14], N. Trotta[66], R. Trotta[13], T. S. Tveter[73], E. Umaka[26], A. Usman[74], H. W. van Hecke[32], J. Velkovska[79], E. Voutier[24], P.K. Wang[24], Q. Wang[69], Y. Wang[8], Y. Wang[63], D. P. Watts[87], L. Weinstein[47], M. Williams[37], C.-P. Wong[32], L. Wood[50], M. H. Wood[7], C. Woody[5], B. Wyslouch[37], Z. Xiao[63], Y. Yamazaki[30], Y. Yang[39], Z. Ye[63], H. D. Yoo[86], M. Yurov[32], N. Zachariou[87], W.A. Zajc[12], J. Zhang[78], Y. Zhang[63], Y. X. Zhao[25], X. Zheng[78], P. Zhuang[63]

[1] *University Of Science And Technology Of China, HeFei, China*
[2] *A. Alikhanyan National Laboratory, Yerevan, Armenia*
[3] *Institute of Physics, Academia Sinica, Taipei, Taiwan*
[4] *Augustana University, , Sioux Falls, , SD, USA*
[5] *Brookhaven National Laboratory, , Upton, 11973, NY, USA*
[6] *Brunel University London, , Uxbridge, , UK*
[7] *Canisius College, , Buffalo, , NY, USA*
[8] *Central China Normal University, Wuhan, China*
[9] *Charles University, Prague, Czech Republic*
[10] *China Institute of Atomic Energy, Fangshan, Beijing, China*
[11] *Christopher Newport University, , Newport News, , VA, USA*
[12] *Columbia University, , New York, , NY, USA*
[13] *Catholic University of America, 620 Michigan Ave., Washington DC, 20064, USA*
[14] *Czech Technical University, , Prague, Czech Republic*
[15] *Duquesne University, , Pittsburgh, , PA, USA*
[16] *Duke University, , , , NC, USA*
[17] *Florida International University, , Miami, , FL, USA*
[18] *Georgia State University, , Atlanta, , GA, USA*
[19] *University of Glasgow, , Glasgow, , UK*
[20] *GSI Helmholtzzentrum fuer Schwerionenforschung, , Darmstadt, , Germany*
[21] *The George Washington University, , Washington, DC, , USA*
[22] *Hampton University, , Hampton, , VA, USA*
[23] *Hebrew University, , Jerusalem, , Isreal*
[24] *Universite Paris-Saclay, CNRS/IN2P3, IJCLab, Orsay, France*
[25] *Chinese Academy of Sciences, , Lanzhou, , , China*
[26] *Iowa State University, , , , IA, USA*
[27] *Jazan University, Jazan, Sadui Arabia*

[28]Thomas Jefferson National Accelerator Facility, 12000 Jefferson Ave., Newport News, 24450, VA, USA
[29]James Madison University, , , , VA, USA
[30]Kobe University, Kobe, Japan
[31]Kyungpook National University, Daegu, Republic of Korea
[32]Los Alamos National Laboratory, , , , NM, USA
[33]Lawrence Berkeley National Lab, , Berkeley, , , USA
[34]Lehigh University, , Bethlehem, , PA, USA
[35]Lawrence Livermore National Laboratory, , Livermore, , CA, USA
[36]Morehead State University, Morehad, KY, USA, , Morehead, , KY, USA
[37]Massachusetts Institute of Technology, 77 Massachusetts Ave., Cambridge, 02139, MA, USA
[38]Mississippi State University, , Mississippi State, , MS, USA
[39] National Cheng Kung University, Tainan, Taiwan, , , , ,
[40]National Central University, Chungli, Taiwan
[41]Nihon University, Tokyo, Japan
[42]New Mexico State University, , Las Cruces, , NM, USA
[43]National Research Nuclear University MEPhI, Moscow, Russian Federation
[44]Nuclear Research Center - Negev, Beer-Sheva, Isreal
[45]National Tsing Hua University, Hsinchu, Taiwan
[46]National Taiwan University, Taipei, Taiwan
[47]Old Dominion University, , Norfolk, , VA, USA
[48]Ohio University, , Athens, , OH, USA
[49]Oak Ridge National Laboratory, PO Box 2008, Oak Ridge, 37831, TN, USA
[50]Pacific Northwest National Laboratory, , Richland, , WA, USA
[51]Pusan National Univeristy, Busan, Republic of Korea
[52]Rice University, P.O. Box 1892, Houston, 77251, TX, USA
[53]RIKEN Nishina Center, Wako, Saitama, Japan
[54]The State University of New Jersey, , Piscataway, , NJ, USA
[55]Center for Frontiers in Nuclear Science, Stony Brook, 11794, NY, USA
[56]Stony Brook University, 100 Nicolis Rd., Stony Brook, 11794, NY, USA
[57]RIKEN BNL Research Center, , Upton, , NY, USA
[58]Seoul National University, Seoul, Republic of Korea
[59]Sejong University, Seoul, Republic of Korea
[60]Shinshu University, Matsumoto, Nagano, Japan
[61]Sungkyunkwan University, Suwon, Republic of Korea
[62]Tel Aviv University, P.O. Box 39040, Tel Aviv, 6997801, Israel
[63]Tsinghua University, Beijing, China
[64]Tsukuba University of Technology, Tsukuba, Ibaraki, Japan
[65]University of Colorado Boulder, Boulder, CO, USA, , Boulder, , CO, USA
[66]University of Connecticut, , Boulder, Storrs, , CT, USA
[67]University of Houston, , Houston, , TX, USA
[68]University of Illinois, , Urbana, , IL, USA
[69]Unviersity of Kansas, 1450 Jayhawk Blvd., Lawrence, 66045, KS, USA
[70]University of Kentucky, , Lexington, 40506, KY, USA
[71]University of Ljubljana, Ljubljana, Slovenia, , Ljubljana, , , Slovenia
[72]University of New Hampshire, , Durham, , NH, USA
[73]University of Oslo, Oslo, Norway
[74] University of Regina, , Regina, , SK, Canada
[75]University of Seoul, Seoul, Republic of Korea
[76]University of Tsukuba, Tsukuba, Japan
[77]University of Tennessee, , Knoxville, , TN, USA
[78]University of Virginia, , Charlottesville, , VA, USA
[79]Vanderbilt University, , Nashville, , TN, USA
[80]Virginia Tech, , Blacksburg, , VA, USA
[81]Virginia Union University, , Richmond, , VA, USA
[82]Wayne State University, , Detroit, , MI, USA
[83]Weizmann Institute of Science, Rehovot, Israel
[84]The College of William and Mary, Williamsburg, VA, USA
[85]Yamagata University, Yamagata, Japan
[86]Yarmouk University, Irbid, Jordan
[87]Yonsei University, Seoul, Republic of Korea
[88]University of York, York, UK
[89]University of Zagreb, Zagreb, Croatia

Abstract

The exclusive heavy quarkonium photoproduction is one of the most popular processes in EIC, which has large cross section and simple final state. Due to the gluonic nature of the exchange Pomeron, this process can be related to the gluon distribution of proton

and nucleus. The momentum transfer dependence of this process is sensitive to the interaction sites, which provides a powerful tool to probe the spatial distribution of gluon in nucleus. And recently the origin of the proton mass problem receive lots of attention on determining the anomaly contribution M_a. The trace anomaly is sensitive to the gluon condensate and exclusive production of quarkonia such as J/ψ and Y is an excellent laboratory to extract it. We present the ECCE Tracking performance of exclusive J/ψ photoproduction detection and the capability of this process to probe the above physics opportunities.

Keywords: ECCE, Electron Ion Collider, Exclusive, Near Threshold, Quarkonia

Contents

1. Introduction

The heavy quakonia is the most simple quark-antiquark bound state, however, its production mechanism is not fully understood yet. Due to the large mass scale, the generation of heavy-antiquark pair can be treated safely by the perturbative QCD, but the later on evolution to heavy quakonia is a soft process, which can only be studied by phenomenal model, such as CEM [1, 2], CSM [3], and NRQCD [4]. The determination of matrix elements for different models rely on the various precise experimental measurements. The electron proton/nucleus collisions constitute an excellent laboratory for the investigations of heavy quarkonia production. The future Electron-Ion Collider (EIC) will provide a much simpler and cleaner environment than hadronic collisions, but far richer than electron-positron annihilation.

Among the heavy quarkonia production processes at EIC, the exclusive photoproduction is expected to play a key role, which has large cross section and simple final state. In the reaction, an incident virtual photon fluctuates into quark-antiquark pair, which then scatters off the target elastically, emerging as a real quarkonium. The scattering process occurs via the exchange of a color neutral object, Pomeron, which can be viewed as two gluons with self interaction (gluon ladder) in the language of QCD. Due to the gluonic nature of Pomeron, the exclusive heavy quarkonia photoproduction at EIC can be related to the gluon distribution of proton and nucleus using perturbative QCD. Furthermore, the distribution of momentum transfer from the target in the process is sensitive to the interaction sites, which provides a powerful tool to probe the spatial distribution of gluon in nucleus.

Nucleons constitute about 99% of the mass of the visible universe. In the standard model, Higgs mechanism describes gauge bosons "mass" generation to some extent, but can only explain a small fraction of the nucleon mass. The other parts come from the strong interaction that binds quarks and gluons together. So understanding the hadron mass decomposition becomes a topic of great interest in QCD. There are two key models[5, 6, 7, 8, 9, 10] for the mass decomposition. One contains a trace anomaly contribution which is quantified by the energy-momentum tensor (EMT) and the other agrees with an energy decomposition in the rest frame of the system. Recently, there has been a lot of interest [11, 12, 13] among the nucleon structure community in determining the anomaly contribution M_a as a key to understand the origin of the proton mass. Specifically, it has been proposed, based on some theory suggestions [14, 15, 16], that one can access M_a through the forward (t=0) cross section via the exclusive production of heavy quarkonium states such as J/ψ and Υ. Heavy quarkonium are of particular interest here because they only couple to gluons, not light quarks, and are therefore sensitive to the gluonic structure of the proton. The trace anomaly is sensitive to the gluon condensate and exclusive production of quarkonia such as J/ψ and Υ is a excellent laboratory to extract the anomaly contribution M_a, in which the sensitivity can be maximized for the production near threshold.

In this paper, we make the single J/ψ simulation by fun4all assumed as exclusive photon produced J/ψ detector response in ECCE tracking system. We make a projection of J/ψ photoproduction in ECCE using the vector dominance model in eSTARLight. And we combine the measurement and projection to give an insight of related fruitful physics opportunities, such as probing gluon nPDF, spatial distribution and proton mass decomposition. The main purpose of this study is to present the capability of exclusive process of J/ψ photoproduction detection and to show the physics opportunities which could be achieved with the ECCE Tracking setup.

2. Simulation Framework and J/ψ Measurement

The ECCE detector is a cylindrical detector covering $|\eta| \leq 3.5$ and the full azimuth. The Tracking and vertexing systems of ECCE are based on semiconductor and gaseous tracking detector technologies. Monolothic Active Pixel Sensor (MAPS) based silicon vertex/tracking detector use ITS-3 technology and μRwell based gas tracker derived from Gas Electron Multiplier (GEM) technology. The momentum resolution of central region and beam e-going direction is closed to or better than the requirement of Yellow Report (YR) [17]

For exclusive photon production of J/ψ, we use eSTARLight to make a projection to the cross section of $ep \rightarrow eJ/\psi p$ pro-

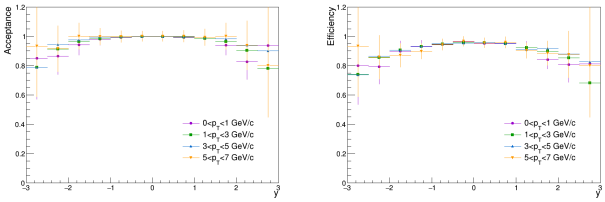

Figure 1: Acceptance and efficiency of single J/ψ simulation

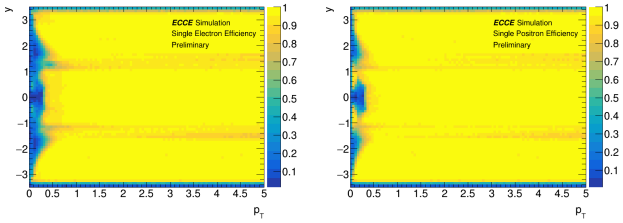

Figure 2: Single track efficiency. Left Panel: e^- efficiency. Right Panel: e^+ efficiency

cess. eSTARLight provides a photo Pomeron interaction model parameterized by HERA data. We study e+p and e+Au collisions for beam configuration 5×41 GeV and 10×100 GeV.

The simulation of the detector response is done using a GEANT4 based package Fun4All. In this work, July detector concept, also known as "Prop.4", is used for J/ψ reconstruction via dielectron channel. Single e^+/e^- Tracking simulation results are as Fig. 2. The difference at very low p_T is due to the initial assumption parameter in Kalman filter. If starting parameter is set "positron", it will get a poor fit quality for different charge (electron), seemed as background. We just set single J/ψ at the zero vertex point and let the daughter particles pass full detector simulation. Here we simulate the tracking acceptance and efficiency of J/ψ as Fig. 1. It is similar to the situation of the exclusive J/ψ photoproduction in the central detector. We also compare different magnitude strength simulation and the tail effect in the mass reconstruction.

The kinematic distribution of J/ψ in exclusive photoproduction is initially projected by the theoretical cross section calculation from eSTARLight. So if J/ψ is put randomly according to the kinematic distribution, the rapidity dependence of total J/ψ reconstruction efficiency of the studied process could be gained from tagging the daughter electron pair according to single track efficiency and reconstruction as Fig. 3. As shown in the figure, the reconstruction efficiency for J/ψ is sufficiently high, about 0.9 in central $|y| < 1.8$ region at ECCE.

We also compare different magnitude strength simulation and the tail effect in the mass reconstruction shown in Fig. 4. At very low p_T ($0.5 < p_T < 1.0$ GeV/c), the improvement of the acceptance of lower magnetic field dominates over the loss of resolution in angle and momentum. while at larger p_T ($1.0 < p_T < 2.0$ GeV/c), 1.4T and 0.7T efficiencies don't show strong difference. And in July Concept, the bremsstrahlung energy loss has already been put in Tracking, which constitutes the tail in reconstruction as (b) in Fig. 4. We scale the tail to

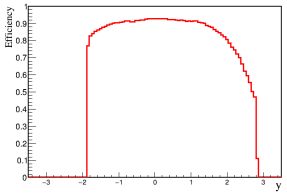

Figure 3: Exclusive J/ψ detection efficiency, steep cliff at backward region is due to upper limit of the emitted photon energy from beam electron. No photo-produced J/ψ thus no meaningful efficiency

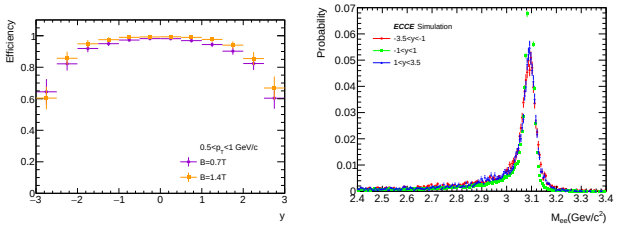

Figure 4: Magnitude strength and tail effect in J/ψ detection

unity and the detail of tail effect can be presented in Table. 1. For three rapidity region of J/ψ in table, forward and backward regions have similar effect contributions a bit larger than the central region. The situation of J/ψ photoproduction lays in forward rapidity region.

Table 1: Tail effect with mass window cut

mass window (GeV/c^2)	$-3.5 < y < -1$	$-1 < y < 1$	$1 < y < 3.5$
2.8-3.2	0.887	0.925	0.890
2.9-3.2	0.833	0.886	0.836
3.0-3.2	0.743	0.814	0.730

3. Theoretical Setup for Projection

In this section, we present the theoretical framework of exclusive J/ψ photoproduction in e+p and e+A collisions, which is employed in our simulation. The cross section $\sigma(eA \to eAV)$ is calculated as an integration of photon flux and the cross section of collision of the virtual photon with the nucleus, shown as Equation(1):

$$\sigma(eA \to eAV) = \int \frac{dW}{W} \int dk \int dQ^2 \frac{d^2N_\gamma}{dkdQ^2} \sigma_{\gamma^* A \to VA}\left(W, Q^2\right) \tag{1}$$

The photon flux can be written as a function of Q^2:

$$\frac{d^2N_\gamma}{dkdQ^2} = \frac{\alpha}{\pi k Q^2}\left[1 - \frac{k}{Ee} + \frac{k^2}{2E_e^2} - \left(1 - \frac{k}{Ee}\right)\left|\frac{Q^2_{\min}}{Q^2}\right|\right] \tag{2}$$

The cross section of collision of the virtual photon with the nucleus is proportional to the cross section at $Q^2 = 0$:

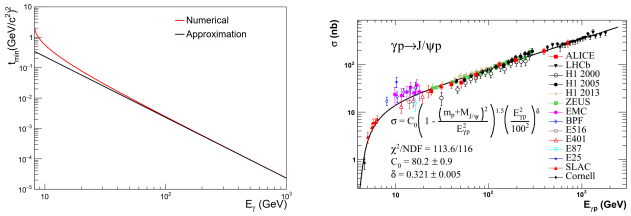

Figure 5: Left Panel: The minimum momentum transfer as a function of incident photon energy. Right Panel: The world-wide measurements of $\sigma(\gamma p \rightarrow Vp)$.

$$\sigma_{\gamma^* A \rightarrow VA}\left(W, Q^2\right) = f\left(M_V\right)\sigma\left(W, Q^2 = 0\right)\left(\frac{M_V^2}{M_V^2 + Q^2}\right)^n \qquad (3)$$
$$n = c_1 + c_2\left(Q^2 + M_V^2\right)$$

Where c_1 and c_2 are constants by fitting from Hera data. And the cross section at $Q^2 = 0$ can be calculated by the integration of the quasi-real photon nucleus scattering cross section and the square of nucleus form factor, revealed as Equation(4):

$$\sigma\left(W, Q^2 = 0\right) = \int_{t_{\min}}^{\infty} dt \frac{d\sigma(\gamma A \rightarrow VA)}{dt}\bigg|_{t=0} |F(t)|^2 \qquad (4)$$

where $\sigma(\gamma A \rightarrow VA)$ can be related to $\sigma(\gamma p \rightarrow Vp)$. The cross section of $\gamma p \rightarrow Vp$ can be parameterized using the world-wide measurements [18]. The framework is almost the same as eSTARLight [19][20], except two minor improvements. In eSTARLight, the minimum momentum transfer t_{min} is approximated as $t_{min} = ((M_v)^2/2k)^2$. We can also calculate the minimum squared four-momentum transfer in collision of a given energy photon and the target proton as the numerical result in Fig. 5. As one can find in the left panel of Fig. 5, the approximation is proper at high energies, however would underestimate the magnitude at low energy range, which is the case for our projection at ECCE. Furthermore, the parametrization of $\gamma p \rightarrow Vp$ cross section in eSTARLight is made only relying on the high energy measurements. As shown in the right panel of Fig. 5, the behaviour of energy dependence is significantly different between the high energy and low energy ranges, which would bias the calculations at EIC. With these two improvements, the calculated results of rapidity distribution for exclusive J/ψ photoproduction in e+p and e+A collisions for 5×41 and 10×100 GeV collision energies are shown in Fig. 6. And Q^2 distribution of e+p collision for 5×41 and 10×100 GeV with a η range in −3 to 3 are illustrated in Fig. 7.

The projected statistics of J/ψ as a function of rapidity are shown in Fig. 8 for e+p and e+Au collisions. For the projection results in the following section, we assume the integrated luminosity collected by ECCE is $100 fb^{-1}$ for e+p collisions and $10 fb^{-1}/A$ for e+Au collisions, where A is the mass number of Au. As shown in the figure, millions of J/ψs would be observed with the designed ECCE setup, which provides us plenty physics opportunities. And Q^2 dependence of the statistics of

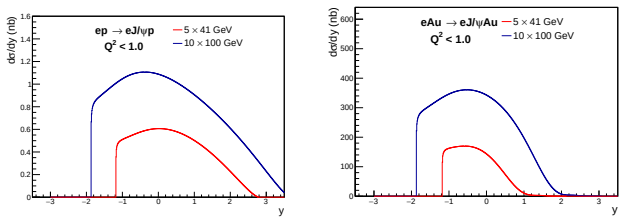

Figure 6: Rapidity dependence of differential cross section of exclusive J/ψ photoproduction

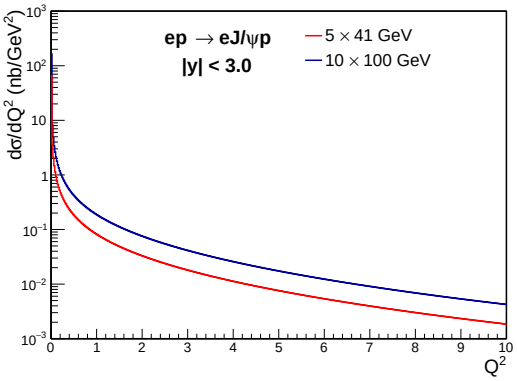

Figure 7: The Q^2 dependence of differential cross section of exclusive J/ψ photoproduction

e+p collision for 5×41 and 10×100 GeV are shown in Fig. 9. As we can see, most of events locate in low Q^2 region, specially for $Q^2 < 1 GeV^2$.

4. Physics Opportunities with Exclusive J/ψ Photoproduction at ECCE

4.1. Probe the Gluon nPDF

The gluon nuclear parton distribution functions (nPDF) in proton and nucleus has large uncertainties, because it does not carry electric charge and can not be directly determined by the DIS measurements. As mentioned in the introduction, the exclusive J/ψ photoproduction occurs via Pomeron exchange, due to the gluonic nature of Pomeron, this process is directly sensitive to the gluon PDF. According to the calculation of perturbative QCD, the forward scattering cross section is proportional

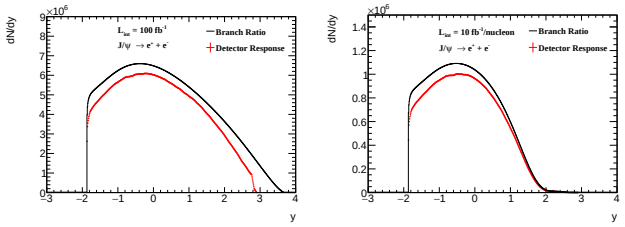

Figure 8: The rapidity distribution of J/ψ amount in e+p and e+A collisions for 10×100 GeV. Left Panel: e+p. Right Panel: e+Au

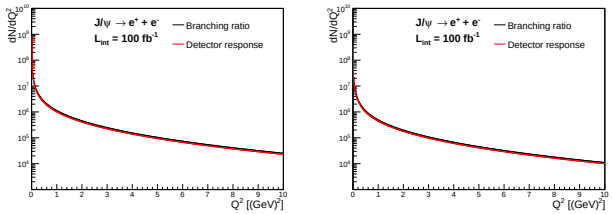

Figure 9: The Q^2 distribution of J/ψ photoproduction in e+p. Left Panel: 10×100 GeV. Right Panel: 5×41 GeV.

to the square of the gluon density distribution, shown as the following[21][22]:

$$\left.\frac{d\sigma(\gamma A \to VA)}{dt}\right|_{t=0} = \frac{\alpha_s^2 \Gamma_{ee}}{3\alpha M_V^5} 16\pi^3 \left[x g_A(x, Q^2)\right]^2 \qquad (5)$$

$$x = \frac{M_V e^{\pm y}}{\sqrt{s}} \qquad Q^2 = M_V^2/4 \qquad R_g = \sqrt{\frac{\left.\frac{d\sigma(\gamma A \to VA)}{dt}\right|_{t=0}}{\left.\frac{d\sigma(\gamma p \to Vp)}{dt}\right|_{t=0}}} \qquad (6)$$

where the momentum fraction x can be determined by the rapidity of J/ψ, and the Q^2 is controlled by the mass of J/ψ. As shown in Equation(6), if we make the forward scattering amplitude ratio between e+p and e+Au collisions, the shadowing factor R_g of gluon can be directly extracted. So measurements of J/ψ photoproduction can provide a direct access to $g_A(x, Q^2)$.

We simulated elastic J/ψ photoproduction processes in 10×100 (GeV) e+p and e+Au collisions with the framework described in the above sections. From the simulation, we extracted the $d^2\sigma/dtdy$ of J/ψ at t =0 for both e+p and e+Au collisions to make projection on R_g. The projection precision is only the statistical error. In an x region, we can transfer it to the corresponding y region through Equation(6), get the statistics with the detector response and signal over background ratio correlation in Fig.8, and randomly select same number of events in the y region. And then we fit the t distribution of differential cross section of these events and get the fit error of $d\sigma/dt$ for e+p and e+Au collisions at $t = 0$. The statistical error can be calculated by the fit error transferred through R_g equation in Equation(6). As shown in Fig.10, EPPS16[23] PDF set has a large uncertainty band, but for most x range covered by ECCE acceptance, the projected statistical error is negligible. This shows the excellent capability of constraining gluon nPDF with the exclusive J/ψ measurements at ECCE.

4.2. Probe the Gluon Spatial Distribution

The Pomeron is the exchange object for diffractive process and diffraction generally is sensitive to gluon spatial distribution. And the momentum transfer from the target in the exclusive J/ψ photoproduction is sensitive to the production site, which provides us a powerful tool to infer the spatial distribution of gluon in both proton and nucleus. In the simulation, we made a projection of t distribution for the processes in 10 × 100 (GeV) e+Au collisions with both coherent and incoherent J/ψ photoproduction. The results

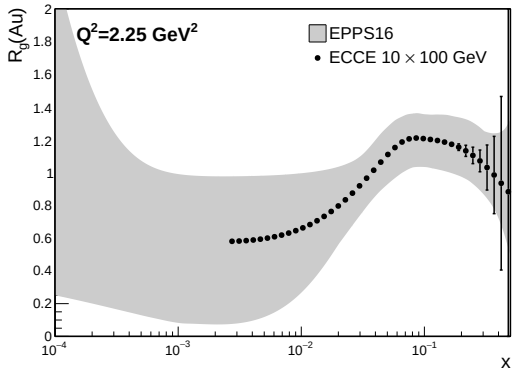

Figure 10: Gluon nuclear shadowing factor as function of momentum fraction x.

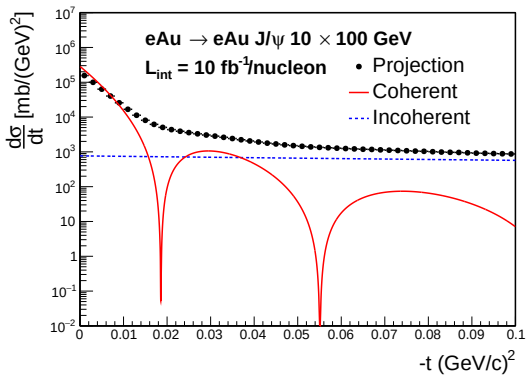

Figure 11: t distribution of exclusive J/ψ production in e+Au collision.

are shown in Fig.11, the red and and blue curves are the coherent and incoherent contributions from calculations, respectively. One can clearly observe the diffraction dips in the coherent contribution, which is related to the size of gluon distribution in nucleus. The solid data points are the projected results from simulation, in which the statistical uncertainty is negligible. However, due to the momentum smearing from the detector, the slope of the distribution is slightly different from that of theoretical calculations and the diffraction dips are fold out. This suggests that the detector response should be precisely determined to extract the gluon spatial distribution.

At low Q^2 0-1 GeV^2 for photoproduction, larger Q^2 1-3 GeV^2 and 3-10 GeV^2, the t distribution is illustrated in Fig. 12 with the systematical error and the statistical error given as Sec.4.1 but not fitting the selected events. The systematical uncertainty is determined by the maximum deviation for truth and the reconstructed distribution. Based on it we can get the relative uncertainty 5% and add it to the plot.

4.3. The Near-Threshold Production Mechanism

For elastic near-threshold J/ψ photoproduction, it can provide a new window into multi-quark, gluonic, hidden-color correlations of hadronic and nuclear wave-functions in QCD. The

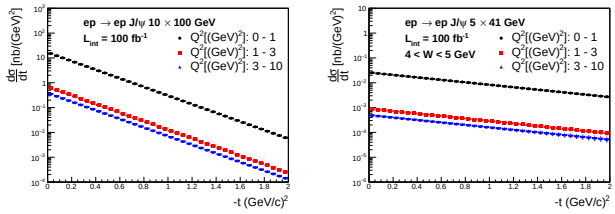

Figure 12: t distribution of exclusive J/ψ production in e+p collision in several Q^2 intervals. Left Panel: 10×100. Right Panel: 5×41

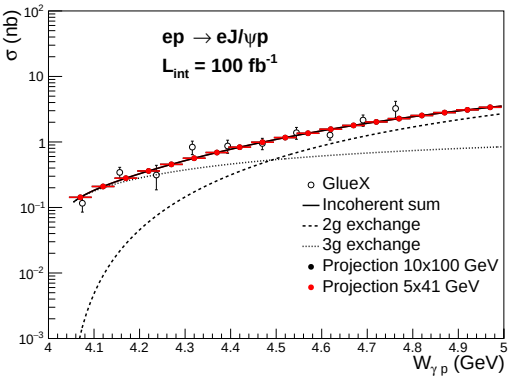

Figure 13: Projection of J/ψ photoproduction cross section near threshold in 10×100 GeV and 5×41 GeV e+p collisions.

near-threshold J/ψ production probes the $x \sim 1$ configuration in the target, the spectator partons carry a vanishing fraction $x \sim 0$ of the target momentum. This implies that the production rate behaves near $x \to 1$ as $(1-x)^{2n_s}$, where n_s is the number of spectators. Then the two gluon and three gluon exchange contributions can be written as [24]:

$$\frac{d\sigma}{dt} = \mathcal{N}_{2g} v \frac{(1-x)^2}{R^2 \mathcal{M}^2} F_{2g}^2(t) \left(W_{\gamma p}^2 - m_p^2\right)^2 \tag{7}$$

$$\frac{d\sigma}{dt} = \mathcal{N}_{3g} v \frac{(1-x)^0}{R^4 \mathcal{M}^4} F_{3g}^2(t) \left(W_{\gamma p}^2 - m_p^2\right)^2 \tag{8}$$

where R is the radius of proton, M is the mass of J/ψ, and $W_{\gamma p}$ is the center of mass energy of γp.

The projected results for near-threshold production for 10×100 GeV and 5×41 GeV ep collisions are shown in Fig. 13. The GlueX results, two and three gluon exchange contributions are also shown for comparison. All the curve and projection results are consistent with the GlueX measurements. The error bars on GlueX measurements represent only statistical uncertainties. In low $W_{\gamma p} < 4.5$ GeV region, cross section is dominated by three gluon exchange process and for $W_{\gamma p} > 4.5$ GeV , two gluon exchange process comes to take control. As shown in the figure, for 10×100 GeV e+p collisions, due to the limited detector coverage, the center of mass energy can only reach as low as 4.5 GeV. But for 5×41 GeV e+p collisions, they cover the whole near-threshold range. The projected statistics is extremely good, which could give strong constraint to the production mechanism near-threshold.

4.4. Trace Anomaly and Proton Mass Decomposition

According to QCD theory, there are four terms of decomposition in nucleon mass as Equation(9)[25]: quark energy M_q, gluon energy M_g, quark mass M_m and the trace anomaly contribution M_a, and these terms are sensitive to the trace anomaly parameter b.

$$\begin{aligned} M_q &= \frac{3}{4}\left(a - \frac{b}{1+\gamma_m}\right) M_N \\ M_g &= \frac{3}{4}(1-a) M_N \\ M_m &= \frac{4+\gamma_m}{4(1+\gamma_m)} b M_N \\ M_a &= \frac{1}{4}(1-b) M_N \end{aligned} \tag{9}$$

Recent theoretical efforts from VMD model and Holographic model [26][27][28] suggest that the trace anomaly parameter can be extracted by the near-threshold exclusive heavy quarkonia process via their production at $\frac{d\sigma}{dt}|t = tmin$. In the simulation, we made the projection of the trace anomaly parameter extraction capability at ECCE. The results are shown in Fig. 14 and Fig. 15, which can provide precise information on the nucleon mass decomposition. The GlueX result[25] of the trace anomaly is also shown for comparison. The projection precision consists of two parts, the statistical error using similar method as Sec. 4.1 and systematical error defined in Sec. 4.2. The $d\sigma/dt|t = 0$ can be related to the trace anomaly parameter with Equation(10,11,12)[25], where $k_{ab}^2 = \left[s - (m_a + m_b)^2\right]\left[s - (m_a - m_b)^2\right]/4s$ denotes the squared momentum of center-of-mass of the corresponding two-body system, Γ is the decay width of specific channel, α is the fine structure constant. $\lambda = \left(p_N p_{J/\psi}/m_{J/\psi}\right)$ is the energy of nucleon in the J/ψ rest frame.

$$\left.\frac{d\sigma_{\gamma N \to J/\psi N}}{dt}\right|_{t=0} = \frac{3\Gamma\left(J/\psi \to e^+e^-\right)}{\alpha m_{J/\psi}} \left(\frac{k_{J/\psi N}}{k_{\gamma N}}\right)^2 \left.\frac{d\sigma_{J/\psi N \to J/\psi N}}{dt}\right|_{t=0} \tag{10}$$

$$\left.\frac{d\sigma_{J/\psi N \to J/\psi N}}{dt}\right|_{t=0} = \frac{1}{64\pi} \frac{1}{m_{J/\psi}^2\left(\lambda^2 - m_N^2\right)} \left|F_{J/\psi N}\right|^2 \tag{11}$$

At low energy, the forward amplitude $F_{J/\psi N}$ can be approximately written as a function of (1-b) in Equation(12, and the relative uncertainty of $d\sigma/dt|t = 0$ can be passed through these transfer formula to get the M_a/M_p ($\propto (1-b)$) uncertainty.

$$\begin{aligned} F_{J/\psi N} &\simeq r_0^3 d_2 \frac{2\pi^2}{27}\left(2M_N^2 - \left\langle N\left|\sum_{i=u,d,s} m_i \bar{q}_i q_i\right|N\right\rangle\right) \\ &\simeq r_0^3 d_2 \frac{2\pi^2}{27}\left(2M_N^2 - 2bM_N^2\right) \\ &\simeq r_0^3 d_2 \frac{2\pi^2}{27} 2M_N^2(1-b) \end{aligned} \tag{12}$$

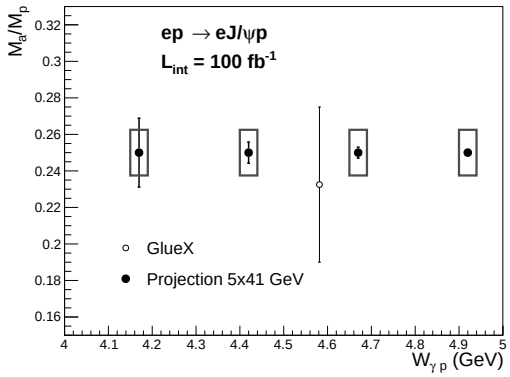

Figure 14: Trace anomaly contribution as a function of γp center of mass energy

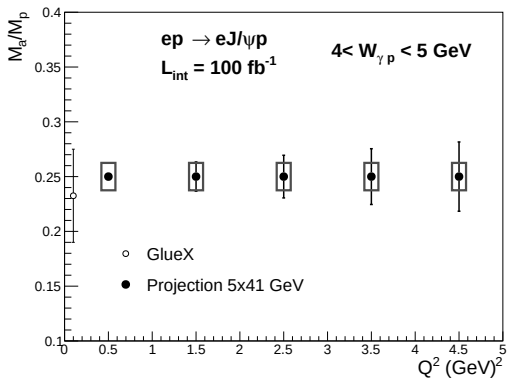

Figure 15: Trace anomaly contribution as a function of Q^2

r_0 is the "Bohr" radius of J/ψ, and d_2 is the Wilson coefficient. While they can just be seen as constant in the relationship of $d\sigma/dt|t = 0$ and $(1-b)$, so the numerical value is not important, cause we use the relative error to give the uncertainty.

5. Summary

In this paper, we make a projection of the exclusive J/ψ photoproduction and its measurement by ECCE Tracking system. The capability of extracting the related physicss opportunities for ECCE can be projected according to the kinematic dependence and the statistic. For J/ψ detection, ECCE has reasonable reconstruction efficiency and coverage, with huge statistics. For gluon distribution in proton and nucleus, the projection of gluon nuclear shadowing effect shows a pretty good capability of constraining the gluon nPDF with the exclusive J/ψ measurements. Then according to the simulation results in Sec.4.3, ECCE can provide a strong constraint to the production mechanism near-threshold. And in Sec.4.4, the measurements of the near-threshold exclusive heavy quarkonia production also shows a good capability of extracting the trace anomaly parameter to provide precise measurements on the nucleon mass decomposition.

References

[1] F. Halzen, Cvc for gluons and hadroproduction of quark flavours, Physics Letters B 69 (1) (1977) 105–108. doi:https://doi.org/10.1016/0370-2693(77)90144-7.
URL https://www.sciencedirect.com/science/article/pii/0370269377901447

[2] H. Fritzsch, Producing heavy quark flavors in hadronic collisions: a test of quantum chromodynamics, Physics Letters B 67 (2) (1977) 217–221. doi:https://doi.org/10.1016/0370-2693(77)90108-3.
URL https://www.sciencedirect.com/science/article/pii/0370269377901083

[3] C. Chao-Hsi, Hadronic production of j/ψ associated with a gluon, Nuclear Physics B 172 (1980) 425–434. doi:https://doi.org/10.1016/0550-3213(80)90175-3.
URL https://www.sciencedirect.com/science/article/pii/0550321380901753

[4] G. T. Bodwin, E. Braaten, G. P. Lepage, Rigorous QCD analysis of inclusive annihilation and production of heavy quarkonium, Phys. Rev. D 51 (1995) 1125–1171, [Erratum: Phys.Rev.D 55, 5853 (1997)]. arXiv:hep-ph/9407339, doi:10.1103/PhysRevD.55.5853.

[5] X. Ji, Qcd analysis of the mass structure of the nucleon, Physical Review Letters 74 (7) (1995) 1071–1074. doi:10.1103/physrevlett.74.1071.
URL http://dx.doi.org/10.1103/PhysRevLett.74.1071

[6] C. Lorcé, On the hadron mass decomposition, The European Physical Journal C 78 (2) (Feb 2018). doi:10.1140/epjc/s10052-018-5561-2.
URL http://dx.doi.org/10.1140/epjc/s10052-018-5561-2

[7] A. Metz, B. Pasquini, S. Rodini, Revisiting the proton mass decomposition, Physical Review D 102 (11) (Dec 2020). doi:10.1103/physrevd.102.114042.
URL http://dx.doi.org/10.1103/PhysRevD.102.114042

[8] C. Roberts, Empirical consequences of emergent mass, Symmetry 12 (9) (2020) 1468. doi:10.3390/sym12091468.
URL http://dx.doi.org/10.3390/sym12091468

[9] K. Tanaka, Three-loop formula for quark and gluon contributions to the qcd trace anomaly, Journal of High Energy Physics 2019 (1) (Jan 2019). doi:10.1007/jhep01(2019)120.
URL http://dx.doi.org/10.1007/JHEP01(2019)120

[10] M. Shifman, A. Vainshtein, V. Zakharov, Remarks on higgs-boson interactions with nucleons, Physics Letters B 78 (4) (1978) 443–446. doi:https://doi.org/10.1016/0370-2693(78)90481-1.
URL https://www.sciencedirect.com/science/article/pii/0370269378904811

[11] X.-D. Ji, Breakup of hadron masses and energy-momentum tensor of QCD, Phys. Rev. D 52 (1995) 271–281. arXiv:hep-ph/9502213, doi:10.1103/PhysRevD.52.271.

[12] X. Ji, Proton mass decomposition: naturalness and interpretations, Front. Phys. (Beijing) 16 (6) (2021) 64601. arXiv:2102.07830, doi:10.1007/s11467-021-1065-x.

[13] Y. Guo, X. Ji, Y. Liu, QCD Analysis of Near-Threshold Photon-Proton Production of Heavy Quarkonium, Phys. Rev. D 103 (9) (2021) 096010. arXiv:2103.11506, doi:10.1103/PhysRevD.103.096010.

[14] S. Brodsky, E. Chudakov, P. Hoyer, J. Laget, Photoproduction of charm near threshold, Physics Letters B 498 (1-2) (2001) 23–28. doi:10.1016/s0370-2693(00)01373-3.
URL http://dx.doi.org/10.1016/S0370-2693(00)01373-3

[15] O. Gryniuk, M. Vanderhaeghen, Accessing the real part of the forward j/ψp scattering amplitude from j/ψ photoproduction on protons around threshold, Physical Review D 94 (7) (Oct 2016). doi:10.1103/physrevd.94.074001.
URL http://dx.doi.org/10.1103/PhysRevD.94.074001

[16] M.-L. Du, V. Baru, F.-K. Guo, C. Hanhart, U.-G. Meißner, A. Nefediev, I. Strakovsky, Deciphering the mechanism of near-threshold j/ψ photoproduction, The European Physical Journal C 80 (11) (Nov 2020). doi:10.1140/epjc/s10052-020-08620-5.
URL http://dx.doi.org/10.1140/epjc/s10052-020-08620-5

[17] R. Abdul Khalek, et al., Science Requirements and Detector Concepts for the Electron-Ion Collider: EIC Yellow Report (Mar 2021). arXiv:2103.05419.

[18] Z.-H. Cao, L.-J. Ruan, Z.-B. Tang, Z.-B. Xu, C. Yang, S. Yang, W.-M. Zha, Photoproduction of j/ψ in non-single-diffractive p+p collisions, Chinese Physics C 43 (6) (2019) 064103. doi:10.1088/1674-1137/43/6/064103.
URL https://doi.org/10.1088/1674-1137/43/6/064103

[19] M. Lomnitz, S. Klein, Exclusive vector meson production at an electron-ion collider, Phys. Rev. C 99 (2019) 015203. doi:10.1103/PhysRevC.99.015203.
URL https://link.aps.org/doi/10.1103/PhysRevC.99.015203

[20] W. Zha, S. R. Klein, R. Ma, L. Ruan, T. Todoroki, Z. Tang, Z. Xu, C. Yang, Q. Yang, S. Yang, Coherent j/ψ photoproduction in hadronic heavy-ion collisions, Phys. Rev. C 97 (2018) 044910. doi:10.1103/PhysRevC.97.044910.
URL https://link.aps.org/doi/10.1103/PhysRevC.97.044910

[21] V. Guzey, M. Zhalov, Exclusive j/ψ production in ultraperipheral collisions at the lhc: constraints on the gluon distributions in the proton and nuclei, Journal of High Energy Physics 2013 (10) (Oct 2013). doi:10.1007/jhep10(2013)207.
URL http://dx.doi.org/10.1007/JHEP10(2013)207

[22] V. Guzey, M. Zhalov, Rapidity and momentum transfer distributions of coherent j/ψ photoproduction in ultraperipheral ppb collisions at the lhc, Journal of High Energy Physics 2014 (2) (Feb 2014). doi:10.1007/jhep02(2014)046.
URL http://dx.doi.org/10.1007/JHEP02(2014)046

[23] K. J. Eskola, P. Paakkinen, H. Paukkunen, C. A. Salgado, Epps16: nuclear parton distributions with lhc data, The European Physical Journal C 77 (3) (Mar 2017). doi:10.1140/epjc/s10052-017-4725-9.
URL http://dx.doi.org/10.1140/epjc/s10052-017-4725-9

[24] S. Brodsky, E. Chudakov, P. Hoyer, J. Laget, Photoproduction of charm near threshold, Physics Letters B 498 (1-2) (2001) 23–28. doi:10.1016/s0370-2693(00)01373-3.
URL http://dx.doi.org/10.1016/S0370-2693(00)01373-3

[25] Wang, Rong, Chen, Xurong, Evslin, Jarah, The origin of proton mass from j/ψ photo-production data, Eur. Phys. J. C 80 (6) (2020) 507. doi:10.1140/epjc/s10052-020-8057-9.
URL https://doi.org/10.1140/epjc/s10052-020-8057-9

[26] K. A. Mamo, I. Zahed, Diffractive photoproduction of j/ψ and υ using holographic qcd: Gravitational form factors and gpd of gluons in the proton, Phys. Rev. D 101 (2020) 086003. doi:10.1103/PhysRevD.101.086003.
URL https://link.aps.org/doi/10.1103/PhysRevD.101.086003

[27] Y. Hatta, D.-L. Yang, Holographic j/ψ production near threshold and the proton mass problem, Phys. Rev. D 98 (2018) 074003. doi:10.1103/PhysRevD.98.074003.
URL https://link.aps.org/doi/10.1103/PhysRevD.98.074003

[28] R. Boussarie, Y. Hatta, Qcd analysis of near-threshold quarkonium leptoproduction at large photon virtualities, Physical Review D 101 (11) (Jun 2020). doi:10.1103/physrevd.101.114004.
URL http://dx.doi.org/10.1103/PhysRevD.101.114004